REVERSIBLE NON-EXPANSIVE SYMMETRIC CONVOLUTION FOR M-CHANNEL LIFTING BASED LINEAR-PHASE FILTER BANKS

Taizo Suzuki

EEE Dept., College of Eng., Nihon University
Koriyama, Fukushima 963-8642, Japan
Email: taizo@ee.ce.nihon-u.ac.jp

Masaaki Ikehara

EEE Dept., Keio University
Yokohama, Kanagawa 223-8522, Japan
Email: ikehara@tkhm.elec.keio.ac.jp

ABSTRACT

This paper presents an effective signal boundary solution in lossy-to-lossless image coding which is the unification of lossy and lossless image coding. Although M-channel filter banks (FBs) for lossy image coding have several effective signal boundary solutions, M-channel lifting based FBs (L-FBs) for lossless image coding do not have such an effective signal boundary solutions due to rounding error in each lifting step. This paper proposes reversible non-expansive symmetric convolution for M-channel lifting based linear-phase FBs (L-LPFBs) to apply lossy-to-lossless image coding. Our proposal is validated by comparing with the periodic extension in lossy-to-lossless image coding.

Index Terms— M-channel lifting based linear-phase filter bank (L-LPFB), lossy-to-lossless image coding, reversible non-expansive symmetric convolution

1. INTRODUCTION

Filter bank (FB) [1] technologies are frequently found in the field of signal processing applications. Especially, M-channel linear-phase FBs (LPFBs) [2], include lapped transforms (LTs) [3], are well-known as one of the most useful transforms for image compression (coding). It is a reason that LPFBs can adopt the symmetric extension [4] to overcome the signal boundary distortion problem. In this approach, the input signals are extended symmetrically in order to maintain the continuity at the signal boundaries. The output signals are reconstructed without the signal boundary distortion by using *symmetry* even if the extended signals are not transmitted. Since the symmetric extension improves the performance of image coding applications, most works in the field of FB systems are focused on LPFBs.

Meanwhile, lifting based LPFBs (L-LPFBs) composed of lifting structures [5] and rounding operations are required for lossy-to-lossless image coding, which is the unification of lossy and lossless image coding, such as JPEG 2000. However, L-LPFBs ($M > 2$) generate the signal boundary distortion because the symmetric extension cannot be applied directly to L-LPFBs due to rounding error. Because of that, the periodic extension is often used for lossy-to-lossless image coding even if the FB without rounding operations has *symmetry* [6].

In this paper, the signal boundary problem in lossy-to-lossless image coding is solved by focusing on *symmetry* in each building block of a particular class of M-channel L-LPFBs again. The proposed reversible symmetric extension can obtain similar smoothness to the symmetric extension at the signal boundaries even if rounding operations are used. Moreover, the computational cost is less due to use of non-expansive convolution [7], i.e., the number of input signals does not increase even temporarily. Our proposal, which this paper calls the reversible non-expansive symmetric convolution, is validated by comparing with the periodic extension in lossy-to-lossless image coding.

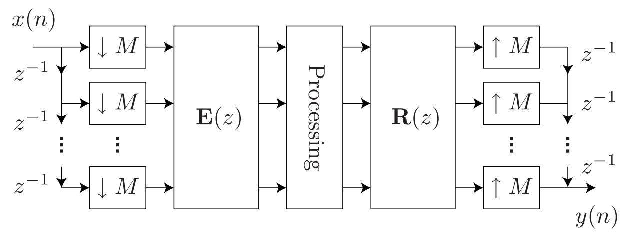

Fig. 1. M-channel FB ($\downarrow, \uparrow$ and z^{-1} means downsampling, upsampling and delay operation, respectively).

Notations: $\mathbf{I}$, $\mathbf{J}$ and $\{\cdot\}^T$ are an identity matrix, a reversal identity matrix and transpose of a matrix, respectively.

2. REVIEW

2.1. Linear-Phase Filter Banks (LPFBs)

The polyphase representation of a typical structure of a FB is shown in Fig. 1. Using the lattice structure, the type-II analysis polyphase matrix $\mathbf{E}(z)$ in an $M \times MK$ LPFB can be presented as [8]

$$\mathbf{E}(z) = \mathbf{E}_0\mathbf{G}_1(z)\cdots\mathbf{G}_{K-2}(z)\mathbf{G}_{K-1}(z) \tag{1}$$

where

$$\mathbf{E}_0 = \mathbf{\Phi}_0\mathbf{W},\ \mathbf{G}_k(z) = \mathbf{\Lambda}(z)\mathbf{\Xi}_k = \mathbf{\Lambda}(z)\mathbf{W}\mathbf{\Phi}_k\mathbf{W},$$
$$\mathbf{\Phi}_k = \begin{bmatrix}\mathbf{U}_k & \mathbf{0}\\ \mathbf{0} & \mathbf{V}_k\end{bmatrix},\ \mathbf{W} = \frac{1}{\sqrt{2}}\begin{bmatrix}\mathbf{I} & \mathbf{J}\\ \mathbf{J} & -\mathbf{I}\end{bmatrix},\ \mathbf{\Lambda}(z) = \begin{bmatrix}\mathbf{I} & \mathbf{0}\\ \mathbf{0} & z^{-1}\mathbf{I}\end{bmatrix}$$

and $\mathbf{U}_k$ and $\mathbf{V}_k$ are $M/2 \times M/2$ arbitrary nonsingular matrices when M is even, respectively. (1) is shown in Fig. 2. Also, $\mathbf{U}_k$ is usually replaced by $\mathbf{I}$ when $k \geq 1$. If $\mathbf{E}(z)$ is invertible, the synthesis polyphase matrix $\mathbf{R}(z)$ can be chosen as the inverse of $\mathbf{E}(z)$, i.e., perfect reconstruction (PR) $\mathbf{R}(z) = \mathbf{E}^T(z^{-1})$ is achieved.

2.2. Lifting Structure

The lifting structure [5], also known as the ladder structure, is a special type of lattice structure. It is implemented by cascading elementary matrices - identity matrices with a single nonzero off-diagonal element.

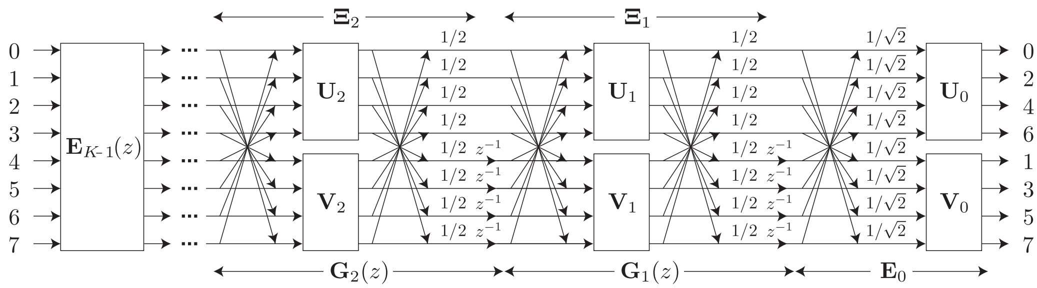

Fig. 2. General lattice structure for $M \times KM$ LPFB (drawn for $M = 8$).

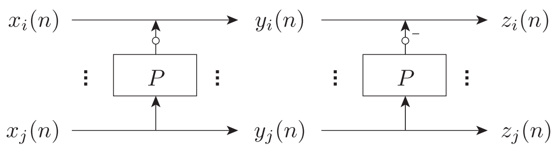

Fig. 3. A lifting structure (white circle: rounding operation).

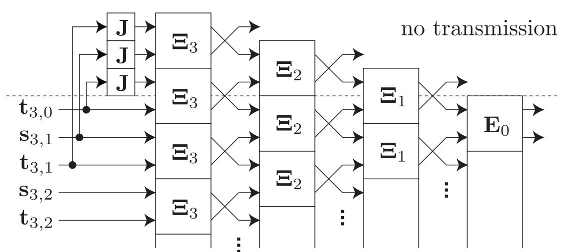

Fig. 4. Analysis part of the symmetric extension by $M \times 4M$ LPFB (dashed line means signal boundary).

Fig. 3 shows a basic lifting structure. It is expressed by

$$\begin{aligned} y_j(n) &= x_j(n), \;\; y_i(n) = x_i(n) + \text{round}\{P x_j(n)\} \\ z_j(n) &= y_j(n), \;\; z_i(n) = y_i(n) - \text{round}\{P y_j(n)\} \end{aligned}$$

where $\text{round}\{\cdot\}$ and P are rounding operation and a lifting coefficient, respectively. Thus the lifting structure with rounding operation can achieve integer-to-integer transform. Also, the lifting matrix and its inverse matrix in this case are represented as

$$\begin{bmatrix} 1 & P \\ 0 & 1 \end{bmatrix} \quad \text{and} \quad \begin{bmatrix} 1 & P \\ 0 & 1 \end{bmatrix}^{-1} = \begin{bmatrix} 1 & -P \\ 0 & 1 \end{bmatrix},$$

respectively.

2.3. Symmetric Extension

In lossy compression without rounding operations, the symmetric extension for LPFB in (1) can be implemented by using *symmetry* in each building block. Fig. 4 shows the analysis part of the symmetric extension in case of $K = 4$. Let l-th ($l \geq 1$) $M \times 1$ input signals for Ξ_k be $\mathbf{X}_{k,l} = \{\mathbf{s}_{k,l}^T, \mathbf{t}_{k,l}^T\}^T$ where $\mathbf{s}_{k,l}$ and $\mathbf{t}_{k,l}$ are $M/2 \times 1$ vectors. If their reflected signals are $\mathbf{J}\mathbf{X}_{k,l}$, *symmetry* is achieved as

$$\Xi_k \mathbf{X}_{k,l} = \Xi_k \begin{bmatrix} \mathbf{s}_{k,l} \\ \mathbf{t}_{k,l} \end{bmatrix} \triangleq \mathbf{Y}_{k,l} \tag{2}$$

$$\Xi_k \mathbf{J}\mathbf{X}_{k,l} = \Xi_k \begin{bmatrix} \mathbf{J}\mathbf{t}_{k,l} \\ \mathbf{J}\mathbf{s}_{k,l} \end{bmatrix} = \mathbf{J}\mathbf{Y}_{k,l} \tag{3}$$

where

$$\mathbf{Y}_{k,l} = \frac{1}{2} \begin{bmatrix} \mathbf{U}_k(\mathbf{s}_{k,l} + \mathbf{J}\mathbf{t}_{k,l}) + \mathbf{J}\mathbf{V}_k(\mathbf{J}\mathbf{s}_{k,l} - \mathbf{t}_{k,l}) \\ \mathbf{J}\mathbf{U}_k(\mathbf{s}_{k,l} + \mathbf{J}\mathbf{t}_{k,l}) - \mathbf{V}_k(\mathbf{J}\mathbf{s}_{k,l} - \mathbf{t}_{k,l}) \end{bmatrix}.$$

Since $\mathbf{s}_{k,0} = \mathbf{J}\mathbf{t}_{k,0}$ when the process is stepping over just signal boundaries, i.e., $l = 0$, the input and output signals are expressed as

$$\mathbf{X}_{k,0} = \begin{bmatrix} \mathbf{J}\mathbf{t}_{k,0} \\ \mathbf{t}_{k,0} \end{bmatrix} = \mathbf{J}\mathbf{X}_{k,0} \;\; \text{and} \;\; \mathbf{Y}_{k,0} = \begin{bmatrix} \mathbf{U}_k \mathbf{J}\mathbf{t}_{k,0} \\ \mathbf{J}\mathbf{U}_k \mathbf{J}\mathbf{t}_{k,0} \end{bmatrix} = \mathbf{J}\mathbf{Y}_{k,0},$$

respectively. In the synthesis part, perfect reconstruction is achieved by using such *symmetry* without receiving redundant signals. As a matter of course, the symmetric extension is also easily applied to the opposite signal boundaries. Note that if the output signals of the input signals $\mathbf{X}_{k,l}$ are $\mathbf{Y}'_{k,l}$ when lifting structures and rounding operations are used in Ξ_k, the output signals of the reflected input signals $\mathbf{J}\mathbf{X}_{k,l}$ are NOT $\mathbf{J}\mathbf{Y}'_{k,l}$ due to rounding error, i.e., *symmetry* is not achieved. Hence, the symmetric extension cannot be directly applied to L-LPFBs.

3. L-LPFBS AND REVERSIBLE NON-EXPANSIVE SYMMETRIC CONVOLUTION

3.1. L-LPFBs

This paper presents L-LPFBs based on [8] and [9]. First, a building block $\mathbf{G}_k(z)$ can be represented by

$$\mathbf{G}_k(z) = \mathbf{\Lambda}(z)\Xi_k \triangleq \mathbf{\Lambda}(z)\mathbf{W}_L \mathbf{\Phi}_k \mathbf{W}_R$$

where

$$\begin{aligned} \mathbf{W}_L &= \mathbf{W} \begin{bmatrix} \frac{1}{\sqrt{2}}\mathbf{I} & \mathbf{0} \\ \mathbf{0} & -\sqrt{2}\mathbf{I} \end{bmatrix} = \begin{bmatrix} \mathbf{I} & \mathbf{0} \\ \mathbf{J} & \mathbf{I} \end{bmatrix} \begin{bmatrix} \mathbf{I} & -\frac{1}{2}\mathbf{J} \\ \mathbf{0} & \mathbf{I} \end{bmatrix} \\ \mathbf{W}_R &= \begin{bmatrix} \sqrt{2}\mathbf{I} & \mathbf{0} \\ \mathbf{0} & -\frac{1}{\sqrt{2}}\mathbf{I} \end{bmatrix} \mathbf{W} = \begin{bmatrix} \mathbf{I} & \frac{1}{2}\mathbf{J} \\ \mathbf{0} & \mathbf{I} \end{bmatrix} \begin{bmatrix} \mathbf{I} & \mathbf{0} \\ -\mathbf{J} & \mathbf{I} \end{bmatrix}. \end{aligned}$$

The half top of Fig. 5 shows a building block Ξ_k of $M \times KM$ L-LPFB. Then, if $\{\hat{\cdot}\}$ means a matrix with rounding operations, $\hat{\mathbf{U}}_k$

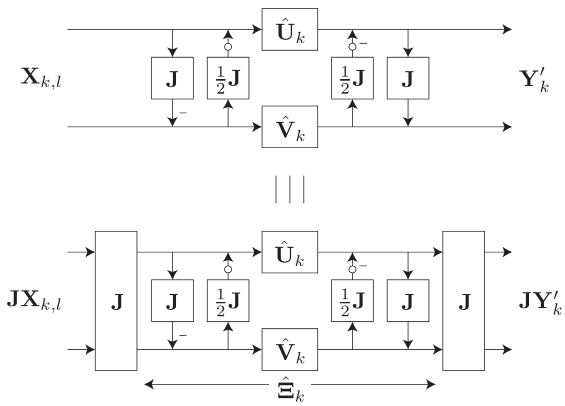

Fig. 5. Building blocks of $M \times KM$ L-LPFB: (top) $\mathbf{\Xi}_k$, (bottom) $\mathbf{J\Xi}_k\mathbf{J}$ for boundary area.

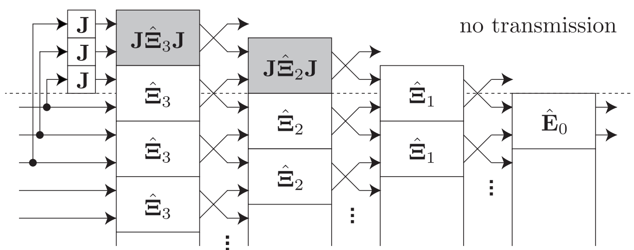

Fig. 6. Analysis part of the reversible symmetric extension by $M \times 4M$ L-LPFB (dashed line means signal boundary).

and $\hat{\mathbf{V}}_k$ mean matrices factorized $\mathbf{U}_k$ and $\mathbf{V}_k$ into single-row elementary reversible matrices (SERMs) by [9] with the fewest rounding operations. Also, $\mathbf{W}$ in the last block $\mathbf{E}_0$ is factorized into lifting structures by lifting factorization of Givens rotation matrix as[1]

$$\mathbf{W} = \begin{bmatrix} \mathbf{I} & (1-\sqrt{2})\,\mathbf{J} \\ \mathbf{0} & \mathbf{I} \end{bmatrix} \begin{bmatrix} \mathbf{I} & \mathbf{0} \\ \frac{1}{\sqrt{2}}\,\mathbf{J} & \mathbf{I} \end{bmatrix} \begin{bmatrix} \mathbf{I} & (1-\sqrt{2})\,\mathbf{J} \\ \mathbf{0} & \mathbf{I} \end{bmatrix} \begin{bmatrix} \mathbf{I} & \mathbf{0} \\ \mathbf{0} & -\mathbf{I} \end{bmatrix}.$$

3.2. Reversible Symmetric Extension

The loss of *symmetry* due to rounding error can be solved by a simple matrix manipulation. Fig.6 shows a realization of *symmetry* with rounding operations.

Case 1 $(l \neq 0)$:

If l-th input signals are $\mathbf{X}_{k,l}$ and rounding operations are considered, it is expressed as

$$\hat{\mathbf{\Xi}}_k \mathbf{X}_{k,l} \triangleq \mathbf{Y}'_{k,l} \neq \mathbf{Y}_{k,l}. \quad (4)$$

According to (2) and (3), $\mathbf{\Xi}_k$ can be represented by

$$\mathbf{\Xi}_k = \mathbf{J\Xi}_k\mathbf{J}.$$

This means that each building block $\mathbf{\Xi}_k$ for extended signals can be replaced by $\mathbf{J\Xi}_k\mathbf{J}$. This relationship is preserved even if $\hat{\mathbf{\Xi}}_k$ is used in place of $\mathbf{\Xi}_k$, i.e.,

$$\hat{\mathbf{\Xi}}_k = \mathbf{J}\hat{\mathbf{\Xi}}_k\mathbf{J}.$$

[1]Although $\mathbf{W}$ in $\mathbf{E}_0$ of biorthogonal LPFB (BOLPFB) can be replaced by $\mathbf{W}_R$, this paper uses paraunitary LPFB (PULPFB) for simplicity.

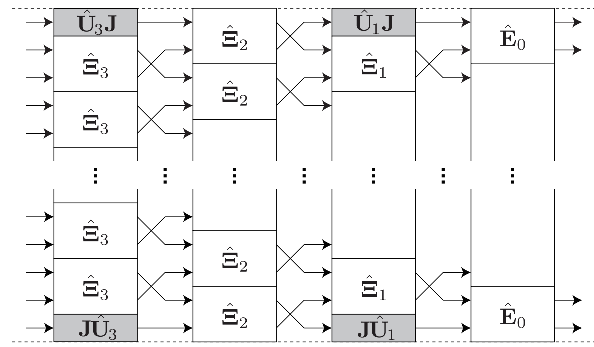

Fig. 7. Analysis part of the reversible non-expansive symmetric convolution by $M \times 4M$ L-LPFB (dashed line means signal boundary).

By the replacement of building blocks on boundary area and (4), the implementation in case of the reflected input signals $\mathbf{JX}_{k,l}$ is similarly expressed as follows:

$$\mathbf{J}\hat{\mathbf{\Xi}}_k\mathbf{J} \cdot \mathbf{JX}_{k,l} = \mathbf{J}\hat{\mathbf{\Xi}}_k\mathbf{X}_{k,l} = \mathbf{JY}'_{k,l}$$

where $\mathbf{J}\cdot\mathbf{J} = \mathbf{I}$. Fig. 5 shows *symmetry* in building blocks $\hat{\mathbf{\Xi}}_k$ and $\mathbf{J}\hat{\mathbf{\Xi}}_k\mathbf{J}$ of $M \times KM$ L-LPFB. As a result, it is clear that *symmetry* can be satisfied by a simple matrix manipulation even if the implementation has rounding operations in case of $l \neq 0$.

Case 2 $(l = 0)$:

This case structurally achieves *symmetry*. Let the input signals $\mathbf{X}_{k,0}$ be $[(\mathbf{Jt}_{k,0})^T, \mathbf{t}_{k,0}^T]^T$ for simplicity. (4) is rewritten as

$$\hat{\mathbf{\Xi}}_k \mathbf{X}_{k,0} = \begin{bmatrix} \hat{\mathbf{U}}_k\mathbf{Jt}_{k,0} \\ \mathbf{J}\hat{\mathbf{U}}_k\mathbf{Jt}_{k,0} \end{bmatrix} = \mathbf{Y}'_{k,0} = \mathbf{JY}'_{k,0}$$

It is clear that *symmetry* is also satisfied even if the implementation has rounding operations in case of $l = 0$.

Consequently, the symmetric extension is applicable to L-LPFBs in (1) by replacing $\hat{\mathbf{\Xi}}_k$ at boundary area to $\mathbf{J}\hat{\mathbf{\Xi}}_k\mathbf{J}$.

3.3. Reversible Non-Expansive Symmetric Convolution

It is important that the input and output signals for $\hat{\mathbf{\Xi}}_k$ always have *symmetry* as already indicated in Sec. 3.2. Additionally, note that only half of the output signals processed by $\hat{\mathbf{\Xi}}_k$ is used in case of $l = 0$, i.e., the signal boundaries. Consequently, the reversible symmetric extension in the above subsection can be replaced by the non-expansive convolution [7] as shown in Fig. 7. This structure, which this paper calls reversible non-expansive symmetric convolution, has less computational cost because it does NOT need extension of the input signals at the signal boundaries temporarily. Also, since $\hat{\mathbf{U}}_k$ $(k \neq 0)$ usually adopts $\mathbf{I}$ as discussed in Sec. 2.1, $\mathbf{J}\hat{\mathbf{U}}_k$ and $\hat{\mathbf{U}}_k\mathbf{J}$ are replaced by simple $\mathbf{J}$.

4. RESULTS

8×16 paraunitary LPFB (PULPFB) and 8×24 PULPFB, which have $\mathbf{U}_k = \mathbf{I}$ $(k \neq 0)$, $\mathbf{U}_0^{-1} = \mathbf{U}_0^T$ and $\mathbf{V}_k^{-1} = \mathbf{V}_k^T$, were designed based on Sec. 3.1 for simplicity. We optimized design parameters by

Table 1. Lossy image coding results (PSNR[dB]).

Test images	9/7-DWT [5]	PULPFB (per.) 8×16	PULPFB (per.) 8×24	PULPFB (prop.) 8×16	PULPFB (prop.) 8×24
bit rate: 0.25 [bpp]					
Barbara	27.28	27.97	28.15	28.09	**28.30**
Elaine	**31.62**	31.01	31.08	31.27	31.35
Finger	23.52	23.60	23.68	23.63	**23.70**
bit rate: 0.50 [bpp]					
Barbara	30.55	31.58	31.73	31.74	**31.92**
Elaine	33.13	32.42	32.56	33.12	**33.17**
Finger	26.02	26.44	26.48	26.49	**26.53**
bit rate:1.00 [bpp]					
Barbara	35.16	35.77	35.75	**35.95**	35.91
Elaine	34.96	34.87	34.82	**35.09**	35.03
Finger	29.15	30.05	30.10	30.09	**30.13**

Table 2. Lossless image coding results (LBR [bpp]).

Test images	5/3-DWT [5]	PULPFB (per.) 8×16	PULPFB (per.) 8×24	PULPFB (prop.) 8×16	PULPFB (prop.) 8×24
Barbara	4.87	4.86	4.88	**4.83**	4.85
Elaine	5.11	5.12	5.12	**5.08**	**5.08**
Finger	5.84	5.71	5.70	5.70	**5.69**

the cost function, which is a weighted linear combination of coding gain, DC leakage and stopband attenuation [1], and `fminunc.m` in `Optimization ToolBox` of `MATLAB`. The resulting PULPFBs were applied to lossy-to-lossless image coding. Integer-to-integer transform can be obtained by using a rounding operation at each lifting step. To evaluate transform performance fairly, a wavelet-based coder EZW-IP [10] was used in the simulation. Also, the reversible non-expansive symmetric convolution and the periodic extension were used for signal boundaries in the designed PULPFBs. In Table 1, we compared the lossy coding results in peak signal-to-noise ratio (PSNR):

$$\mathrm{PSNR}\ [\mathrm{dB}] = 10 \log_{10} \left(\frac{255^2}{\mathrm{MSE}} \right)$$

where MSE is the mean squared error, at 0.25, 0.50 and 1.00 bit per pixel (bpp) for several 512×512 8-bit grayscale images as *Barbara*. The bolds mean the best PSNRs. 9/7-tap discrete wavelet transform (9/7-DWT) is used in JPEG 2000 lossy mode. Fig. 8 illustrates the comparison of a particular area of the image *Barbara*. In signal boundaries shown in each right side of Fig. 8, it is obvious that the proposed non-expansive convolution is better than the periodic extension.[2]

Since the proposed PULPFBs are integer-to-integer transforms, we can also obtain lossless reconstructed images at high bit rate. Lossless coding performance in lossless bit rate (LBR) [bpp]:

$$\mathrm{LBR}\ [\mathrm{bpp}] = \frac{\text{Total number of bits [bit]}}{\text{Total number of pixels [pixel]}}$$

is shown in Table 2. The bolds mean the best LBRs. 5/3-tap DWT (5/3-DWT) is used in JPEG 2000 lossless mode. Similar to the lossy image coding results, the proposed L-LPFBs show the effectiveness for the images with high frequency components.

[2]Fig. 8 shows a particular area of the image *Barbara*. The left side, top and bottom of Fig. 8 are NOT boundaries.

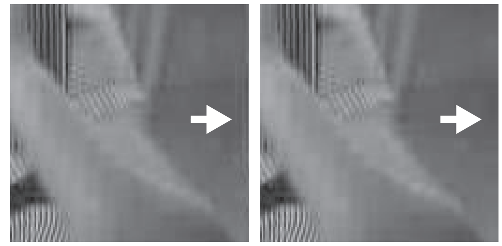

Fig. 8. Comparison of a particular area of the image *Barbara* reconstructed by 8×24 PULPFBs (bit rate: 0.25[bpp]): (left) the periodic extension, (right) the proposed method.

5. CONCLUSION

This paper presented the reversible non-expansive symmetric convolution for M-channel lifting based linear-phase filter banks (L-LPFBs) to apply lossy-to-lossless image coding. Since the proposed method has similar smoothness to the symmetric extension at the signal boundaries, it does NOT generate the signal boundary distortion even if rounding operations are used. Moreover, the computational cost is less due to non-expansive convolution. As result, it achieved better coding performance than the periodic extension.

6. REFERENCES

[1] P. P. Vaidyanathan, *Multirate Systems and Filter Banks*, Englewood Cliffs, NJ: Prentice Hall, 1992.

[2] T. D. Tran, R. L. de Queiroz, and T. Q. Nguyen, “Linear-phase perfect reconstruction filter bank: Lattice structure, design, and application in image coding,” *IEEE Trans. Signal Process.*, vol. 48, no. 1, pp. 133–147, Jan. 2000.

[3] H. S. Malvar, “Lapped transforms for efficient transform/subband coding,” *IEEE Trans. Acoust., Speech, Signal Process.*, vol. 38, no. 6, pp. 969–978, June 1990.

[4] M. J. T. Smith and S. L. Eddins, “Analysis/synthesis techniques for subband image coding,” *IEEE Trans. Signal Process.*, vol. 38, no. 8, pp. 1446–1456, Aug. 1990.

[5] I. Daubechies and W. Sweldens, “Factoring wavelet transforms into lifting steps,” *J. Fourier Anal. Appl.*, vol. 4, no. 3, pp. 245–267, 1998.

[6] T. Suzuki and M. Ikehara, “Integer fast lapped orthogonal transform based on direct-lifting of DCTs for lossless-to-lossy image coding,” in *Proc. of ICASSP’11*, Prague, Czech Republic, May 2011, pp. 1525–1528.

[7] T. Nagai, M. Ikehara, M. Kaneko, and A. Kurematsu, “Generalized unequal length lapped orthogonal transform for subband image coding,” *IEEE Trans. Signal Process.*, vol. 48, no. 12, pp. 3365–3378, Dec. 2000.

[8] T. D. Tran, “M-channel linear phase perfect reconstruction filter bank with rational coefficients,” *IEEE Trans. Circuits Syst. I*, vol. 49, no. 7, pp. 914–927, July 2002.

[9] P. Hao and Q. Shi, “Matrix factorizations for reversible integer mapping,” *IEEE Trans. Signal Process.*, vol. 49, no. 10, pp. 2314–2324, Oct. 2001.

[10] Z. Liu and L. J. Karam, “An efficient embedded zerotree wavelet image codec based on intraband partitioning,” in *Proc. of ICIP’00*, Vancouver, British Columbia, Canada, Sep. 2000.